B-N Lewis Pair-Fused Dipyridylfluorene Copolymers Incorporating Electron-Deficient Benzothiadiazole Comonomers

Abdullah F. Alahmadi, Jingyao Zuo, and Frieder Jäkle*

Department of Chemistry, Rutgers University-Newark, 73 Warren Street, Newark, NJ 07102, USA

* Corresponding Author: Frieder Jäkle (email: fjaekle@rutgers.edu)

Running Head: *B-N Lewis Pair-Fused Copolymers*

Abstract: The isosteric replacement of C-C with B-N units is emerging as a powerful method to tune the optoelectronic properties of organic π-conjugated materials. In this work, copolymers based on a ladder-type B-N Lewis pair-fused dipyridylfluorene monomer and a thienylated benzothiadiazole (BTDDT) are prepared by Stille-type polycondensation. The polymers containing exocyclic ethyl or pentafluorophenyl substituents on boron are characterized by multinuclear NMR spectroscopy and gel permeation chromatography, which provides estimates of the average degrees of polymerization (DP_n) of 30 (R = Et) and 10 (R = C_6F_5). Electrochemical analyses on thin films reveal two distinct reversible reductions that are assigned to benzothiadiazole and boron-fused dipyridylfluorene centered processes respectively. UV-vis analyses show that the band gaps are significantly lowered relative to both BTDDT and the boron-containing monomers. As a result, the absorption and emission bands are shifted to much lower energies, leading to intense orange emission with maxima at 641 nm (R = Et) and 627 nm (R = C_6F_5) respectively with quantum yields of over 50%. Computational studies on molecular model dyads offer insights into the effects of the isosteric replacement of C-C units in ladder-type fused bisfluorene with B-N Lewis pairs on the electronic structures of the polymers.

Keywords: Benzothiadiazole / Boron / Boron Polymer / Lewis Pair / Luminescence

Introduction

The design and synthesis of innovative conjugated materials through isosteric substitution of B-N for C-C units is garnering intense research interest because properties that are distinct from those of the respective hydrocarbon-based systems can be realized.[1-3] Much effort has been focused on embedding B-N units within polycyclic aromatic hydrocarbons (PAHs) and, in dependence on the specific sites in which boron and nitrogen are placed, the modulation of the electronic structure and tuning of intermolecular interactions.[4-9] This research has led to significant advances in application fields ranging from field effect transistors to photovoltaics, development of new battery materials to catalytically active materials for oxygen reduction and hydrogen evolution processes, and applications in biological imaging to the development of enzyme inhibitors.[10] In most of these materials, the boron and nitrogen atoms are found in a trigonal planar environment, taking the place of sp^2-hybridized carbon atoms. Researchers have also explored the functionalization of organic (hetero)aromatic and polycyclic aromatic hydrocarbons with B←N Lewis pairs, in which interactions between the lone pair on nitrogen of N-heterocycles and the empty p-orbital on boron result in a tetracoordinate environment at boron.[11-25] Such dynamic B←N interactions not only allow for planarization of adjacent (hetero)aromatic π-systems, and thereby the effective extension of π-conjugation, but also lead to polarization of the molecules due to the electron withdrawing character of the borane Lewis acid.[26,27] Recently, this concept has also been applied to the design of new functional polymeric materials, attracting particular interest in the fields of light emitting, stimuli-responsive, and acceptor materials for all-polymer solar cells.[28-36]

In prior work, we have pursued the functionalization of various polyaromatic systems with B←N Lewis pairs by N-directed electrophilic borylation of pyridyl-functionalized polyaromatics, including dipyridylfluorene-, dipyridylanthracene- and dipyridylpyrene-based systems.[37-42] In one example, we demonstrated that the borylative fusion of dipyridylfluorene gives rise to strongly emissive ladder-type conjugated molecules in which the B←N Lewis pair formation results in planarization and rigidification of the dipyridylfluorene building block.[37] The blue-emissive B-N fused fluorene ladder compounds were successfully incorporated into conjugated polymers, Poly(BNEt) and Poly(BNEt-coVi), by transition metal-catalyzed C-C coupling reaction.[39] Extension of π-conjugation resulted in polymeric materials that show strong green fluorescence in solution and in the solid state.

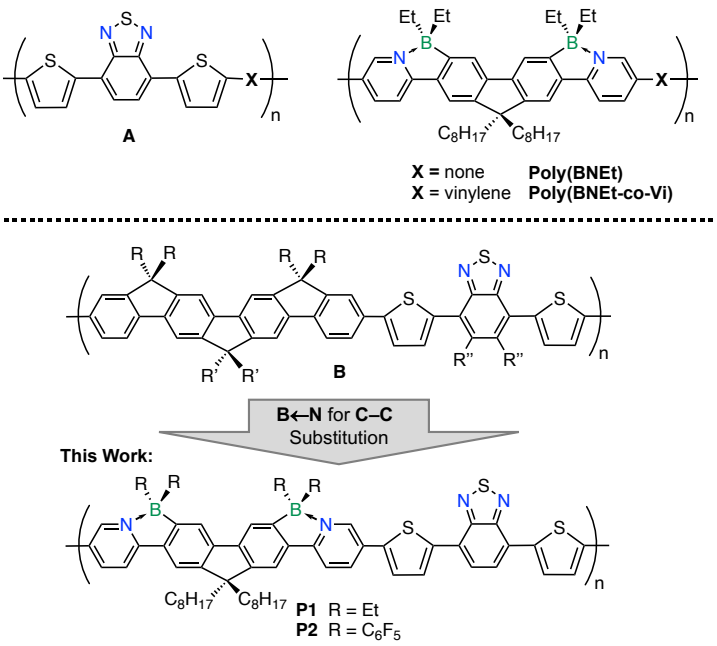

Figure 1. (Top) Examples of benzothiadiazole-based and ladder-type B←N Lewis pair-fused dipyridylfluorene polymers; (bottom) design of new polymers **P1** and **P2** via B←N for C-C substitution.

We were interested in exploring how the combination of these boron-fused dipyridylfluorenes with electron-deficient acceptor-type comonomers would affect the electronic structure and emissive properties of the resulting copolymers. An acceptor building block that is commonly used in the design of donor-π-acceptor copolymers is benzothiadiazole (BTD). As illustrated in Figure 1, BTD is readily incorporated into alternating copolymers with fluorene as electron-rich component by using thiophene linkers to promote electronic delocalization. In these polymers BTD can act as an ambipolar building block in and of itself because intramolecular charge transfer occurs from the electron-rich dithienylbenzene to the electron-deficient thiadiazol subunit.[43,44] BTD copolymers of this kind have been explored in diverse application fields, ranging from photovoltaics to emissive materials, photocatalytic hydrogen evolution, and tumor imaging.[45-52] Thus, we designed and synthesized a new class of copolymers that combine boron-fused dipyridylfluorene ladder compounds with BTD (**P1** and **P2**, Figure 1). Polymers **P1** and **P2** are isosteric analogs of copolymers **B**[53] (Figure 1) that are composed of electron-deficient BTD units in combination with electron-rich fused bisfluorenes. However, different from the all-carbon systems, the B←N Lewis pair functionalization in **P1** and **P2** results in a polarized

microenvironment while also adding an additional element of tunability by varying the Lewis acid strength of the organoborane Lewis acid component. The effects of this "B-N for C-C" substitution on the electronic structure are explored experimentally and through computational studies on molecular dyads comprising a single BTDDT unit linked to a BN-doped ladder-type bisfluorene.

Experimental Section

Materials and Methods. $Pd_2(dba)_3$ and P(*o*-tolyl)$_3$ were purchased from commercial sources and used without further purification. Pentafluorophenyl copper (CuC_6F_5), BNBr, BNEt and BTDDT-Sn were synthesized according to literature procedures.[37,39,54-56] The solvents were dried and degassed prior to use. All reactions were carried out under nitrogen atmosphere using either Schlenk techniques or an inert-atmosphere glove box. The products are air stable and were isolated under ambient conditions.

NMR spectra were acquired at 25 °C on a Bruker Avance III HD NMR spectrometer at operating frequencies of 500.2 MHz (^{1}H), 160.4 MHz (^{11}B) and 470.7 MHz (^{19}F) or a Varian NMR spectrometer at operating frequencies of 599.7 MHz (^{1}H) and 150.8 MHz (^{13}C). ^{11}B NMR spectra were acquired on the Bruker Avance III HD NMR spectrometer with a 5mm PH SEX 500S1 ^{11}B-H/F-D probe using boron-free quartz NMR tubes. ^{1}H and ^{13}C NMR spectra were referenced internally to solvent signals ($CDCl_3$: 7.27 ppm for residual protonated $CHCl_3$ in ^{1}H and 77.0 ppm for ^{13}C NMR spectra) and all other NMR spectra externally (trifluorotoluene $\delta(^{19}F)$ = -63.72 ppm, BF_3•Et_2O $\delta(^{11}B)$ = 0 ppm). Abbreviations used for signal assignments: Py = pyridyl, Fl = fluorenediyl, Th = thienylene, Pf = pentafluorophenyl, BTD = benzothiadiazole, s = singlet, d = doublet, m = multiplet, br = broad.

High-resolution atmospheric pressure chemical ionization mass spectrometry (APCI-MS) data were obtained in negative mode on an Apex Ultra 7.0 Hybrid FTMS. GPC analyses were performed in THF (1.0 mL min^{-1}, 35 ℃; PLgel 5 µm guard, Plgel 5 µm MIXED-C, Plgel 5 µm MIXED-D columns from Polymer Laboratories) using a Waters Alliance GPC solvent/sample module equipped with a 717plus autosampler, a 1525 binary HPLC pump, a 2414 refractive index detector, and a 2600 PDA detector). Samples were dissolved in THF aided by sonication and filtered prior to analysis. The system was calibrated against narrow polystyrene standards (10) in the molecular weight range of 580 to 371,100 Da.

UV-visible absorption data were acquired on a Varian Cary 5000 UV-Vis/NIR spectrophotometer. The fluorescence data and lifetimes were measured in air using a Horiba Fluorolog-3 spectrofluorometer with a nanoLED (450 nm) for excitation and a FluoroHub R-928 detector for time-resolved single-photon counting. Absolute quantum yields were measured on the HORIBA Fluorolog-3 using a pre-calibrated Quanta-φ integrating sphere. Light from the sample compartment is directed into the sphere through a fiber-optic cable and a F-3000 Fiber-Optic Adapter, and then returned to the sample compartment (and to the emission monochromator) through a second fiber-optic cable. A 4-curve method using a Thorlabs neutral density filter was applied.

Cyclic voltammetry (CV) experiments were carried out on a BASI CV-50 W analyzer. The three-electrode system consisted of a gold disk as working electrode, a Pt wire as secondary electrode, and an Ag wire as the pseudo-reference electrode. Thin films of the polymers were drop-cast onto the Au electrode and voltammograms were recorded in acetonitrile solutions containing $Bu_4N[PF_6]$ (0.1 M) as the supporting electrolyte and referenced to ferrocene as internal standard.

DFT calculations were performed with the Gaussian16 suite of programs.[57] The input files were generated in Chem3D and the structures pre-optimized in Spartan ‘08 V 1.2.0. Ground state geometries were then optimized in Gaussian16 using the hybrid density functional RB3LYP with a 6-31G(d) basis set. Frequency calculations were performed to confirm the presence of local minima (only positive frequencies). Vertical excitations were calculated by TD-DFT methods at the rcam-B3LYP/6-31G(d) level.

Synthesis of Monomer BNPf. In a glovebox under nitrogen atmosphere, BNBr (550 mg, 528 μmol) was added to a flame-dried Schlenk flask and dissolved in 50 ml of toluene. Pentafluorophenyl copper (608 mg, 2.64 mmol, 5 equiv) was dissolved in 25 ml of toluene and added to the BNBr solution. The mixture was kept stirring for 3 days. The solution was passed through a short plug of silica on a fritted funnel, and the solvent was removed from the filtrate under reduced pressure. The collected solid was then redissolved in DCM and the solution layered with acetonitrile. The slow diffusion of solvent led to precipitation of the product, BNPf, as a yellow powder. Yield: 0.178 g (24%). ^{1}H NMR (500.2 MHz, $CDCl_3$, δ): 8.59 (s, 2H, Py), 8.24 (dd, 2H, J = 8.8, 2.0 Hz, 2H, Py) 8.02 (s, 2H, Fl), 8.00 (d, 2H, J = 8.5 Hz, Py), 7.75 (s, 2H, Fl), 2.05 (m, 4H, alkyl-H), 1.15 (m, 4H, alkyl-H), 1.12-1.02 (m, 20H, alkyl-H), 0.78 (t, J = 7.2 Hz, 6H, alkyl-H), 0.67 (m, 4H, alkyl-H); ^{13}C[^{1}H] NMR (150.8 MHz, $CDCl_3$, δ): 157.9, 156.4 (br), 151.5,

147.8 (br d, $^{1}J(^{13}C,^{19}F)$ = 239 Hz), 145.5, 144.9, 139.9 (br d, $^{1}J(^{13}C,^{19}F)$ = 252 Hz), 137.2 (br d, $^{1}J(^{13}C,^{19}F)$ = 256 Hz), 134.4, 122.4, 119.3, 117.1 (br), 116.9, 116.1, 54.6, 40.8, 31.7, 29.9, 29.1 (2 signals), 23.7, 22.5, 14.0; ^{19}F NMR (470.7 MHz, $CDCl_3$, δ): −131.7 (m, 8F, *ortho*-Pf), −156.95 (t, $J(^{19}F,^{19}F)$ = 20.3 Hz, 4F, *para*-Pf), −162.61 (m, 8F, *meta*-Pf); $^{11}B[^{1}H]$ NMR (160.4 MHz, $CDCl_3$, δ): -1.5 ($w_{1/2}$ = 920 Hz). HRMS (APCI in CH_2Cl_2, neg. mode) *m*/*z* = 1390.1794 ($[M]^-$, calcd for $^{12}C_{63}{}^{1}H_{44}{}^{11}B_2{}^{79}Br^{81}Br{}^{19}F_{20}{}^{14}N_2$ 1390.1738). UV-Vis (*THF*): λ_{abs} = 416 nm; fluorescence (*THF*, λ_{exc} = 416 nm): λ_{Fl} = 451 nm.

Synthesis of Polymer P1. In a glovebox, under nitrogen atmosphere, BNEt (210.0 mg, 250.5 µmol) and BTDDT-Sn (220.0 mg, 250.4 µmol) were added to a flame-dried Schlenk flask and dissolved in 10 ml of dry toluene. $Pd_2(dba)_3$ (6.9 mg, 3 mol%) and P(o-tolyl)$_3$ (13.8 mg, 18 mol%) were dissolved in 5 ml of dry toluene and added to the monomer solution. The mixture was heated to 110 ºC for 24 hrs. The mixture was allowed to cool to room temperature, diluted with 5 ml of THF and added dropwise to 150 ml of methanol. After centrifuging the product was collected as a red solid. The crude polymer was extracted several times with toluene to remove low molecular weight oligomers. The polymer **P1** was collected as a poorly soluble red solid and dried under vacuum. Yield: 126 mg (51%). ^{1}H NMR (500.2 MHz, $CDCl_3$, δ): 8.69 (br s, Py), 8.26 (br d, Py), 8.23 (br, Th), 8.12 (br s, Fl), 8.07 (br d, Py), 8.04 (br s, BTD), 7.79 (br s, Fl), 7.60 (br, Th), 2.05 (br, alkyl-H), 1.15 – 0.35 (m, alkyl-H); $^{11}B[^{1}H]$ NMR (160.4 MHz, $CDCl_3$, δ): 2.7 ($w_{1/2}$ = 1500 Hz); GPC (*THF*, 1 mL min^{-1}): M_n = 29480, M_w = 68890, $Đ$ = 2.34, DP_n = 30; UV-Vis (*THF*): λ_{abs} = 516 nm; fluorescence (*THF*, λ_{exc} = 516 nm): λ_{Fl} = 641, 430 nm.

Synthesis of Polymer P2. In a glovebox, under nitrogen atmosphere, BNPf (102.0 mg, 73.4 µmol) and BTDDT-Sn (64.5 mg, 73.4 µmol) were added to a flame-dried Schlenk flask and dissolved in 10 ml of dry toluene. $Pd_2(dba)_3$ (2.0 mg, 3 mol%) and P(o-tolyl)$_3$ (4.0 mg, 18 mol%) were dissolved in 5 ml of dry toluene and added to the monomer solution. The mixture was heated to 110 ºC for 24 hrs. The mixture was cooled to room temperature, diluted with 5 ml THF and added dropwise to 150 ml methanol. After centrifuging the product was collected as a red solid. The crude polymer was extracted several times with toluene to remove low molecular weight oligomers. The polymer **P2** was collected as a red solid and dried under vacuum. Yield: 32 mg (29%). ^{1}H NMR (500.2 MHz, $CDCl_3$, δ): 8.84 (br s, Py), 8.39 (br d, Py), 8.18 (br, Th), 8.15 (m, Py), 8.07 (br s, Fl), 8.00 (br s, BTD), 7.96/7.94 (2 × d, BTD end group), 7.81 (br s, Fl), 7.53 (br m, Th with end groups), 2.1 (br, alkyl-H), 1.3-1.0 (m, alkyl-H), 0.9-0.7 (m, alkyl-H); ^{19}F NMR (470.7

MHz, $CDCl_3$, δ): −131.7 (br, 8n F, *ortho*-Pf), −157.3 (br, 4n F, *para*-Pf), −162.8 (br, 8n F, *meta*-Pf); $^{11}B[^1H]$ NMR (160.4 MHz, $CDCl_3$, δ): -3.4 ($w_{1/2}$ = 800 Hz); GPC (*THF*, 1 mL min^{-1}): M_n = 16680, M_w = 24540, $Đ$ = 1.47, DP_n = 10; UV-Vis (*THF*): λ_{abs} = 508, 443 (sh) nm; fluorescence (*THF*, λ_{exc} = 508 nm): λ_{Fl} = 627 nm.

Results and Discussion

The synthetic route to the monomers is outlined in Scheme 1. 4,7-Dithieny-2-yl benzodithiadiazole (BTDDT) was synthesized by Stille coupling of 2-trimethylstannyl thiophene and 4,7-dibromo benzothiadiazole according to a literature procedure.[56] The crude product was purified by silica gel column chromatography using a 1:1 hexanes:DCM mixture as the eluent to give the pure product as red crystals in 61% yield. BTDDT was then converted to the distannylated species BTDDT-Sn by lithiation using LDA, followed by addition of tributylstannyl chloride.[56] Spectroscopically pure BTDDT-Sn was obtained as red oil in 93% yield after purification by silica gel column chromatography using 10% triethylamine in hexanes as eluent. The B-N Lewis pair monomer BNEt (R = Et) was obtained in 62% yield by reacting the brominated precursor BNBr with $ZnEt_2$ according to a previously reported procedure.[39] Reaction of BNBr with CuC_6F_5 in toluene gave the new monomer BNPf which was isolated in 24% yield by precipitation, induced by addition of acetonitrile to a solution in dichloromethane.

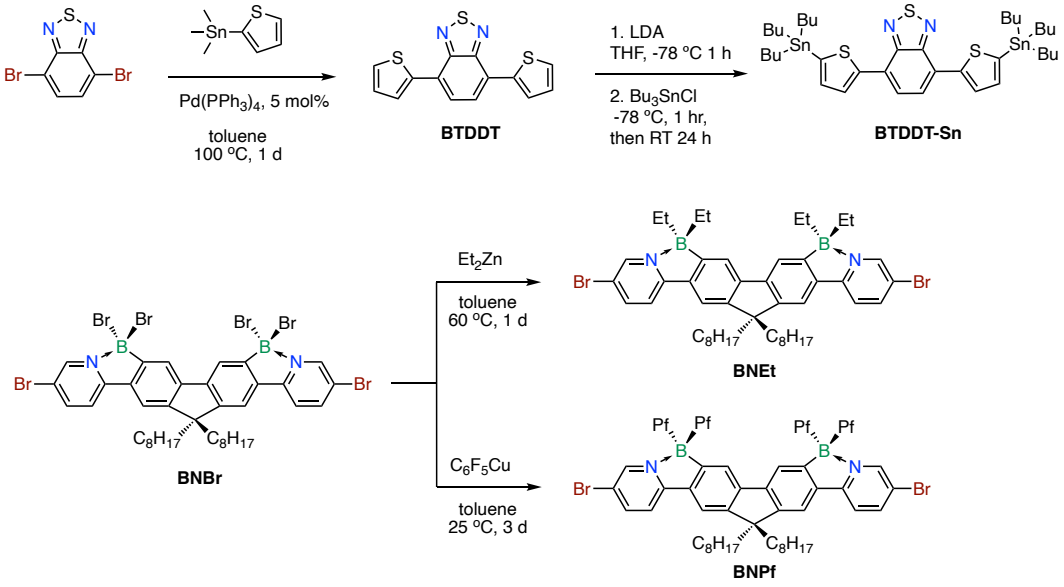

Scheme 1. Synthesis of monomers.

The polymers were synthesized by Stille coupling of BTDDT-Sn and the respective BN Lewis pair monomer (Scheme 2). The resulted polymers **P1** (R = Et) and **P2** (R = Pf) were precipitated in methanol and collected by centrifugation. To remove low molecular weight oligomers the collected solids were extracted several times with toluene. The pure polymers **P1** (51% yield) and **P2** (29% yield) were isolated as red powdery solids and dried under high vacuum.

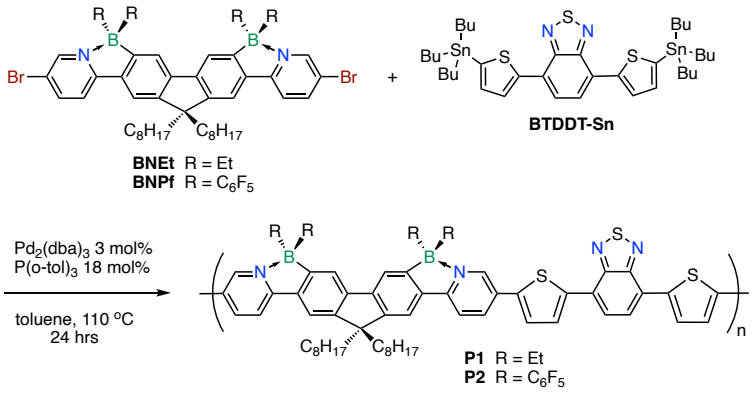

Scheme 2. Synthesis of polymers by Stille coupling polymerization.

The ^{1}H NMR spectra of the polymers feature patterns that are broadened and downfield shifted relative to those of the monomers, BNEt and BNPf, as a result of electronic coupling with the electron-deficient BTD units. For example, the NMR signal for the C-H adjacent to the pyridine-nitrogen shifted from 8.43 for BNEt to 8.69 ppm for **P1** and from 8.59 for BNPf to 8.84 ppm for **P2**. As illustrated in Figure 2, signals for the constituting BTDDT units and B-N Lewis pair monomers could be fully assigned based on 2D H,H-COSY, H,H-TOCSY and H,H-NOESY NMR spectra (Supporting Information), confirming their incorporation into the alternating copolymer structures. ^{11}B NMR spectra of polymers **P1** and **P2** show signals at 2.7 (BNEt: 4.0 ppm) and -3.4 ppm (BNPf: -1.5 ppm), respectively, confirming the presence of tetracoordinate boron centers. The intact structure of the pyridyl-bound $B(C_6F_5)_2$ groups in **P2** was further verified by comparison of the ^{19}F NMR signals with those for the monomer BNPf. A single set of broadened signals is detected at -131.7, -157.3, -162.8 ppm for the *ortho*-, *para*- and *meta*-fluorines at very similar chemical shifts as those of the precursor BNPf (-131.7, -157.0, -162.6 ppm). GPC analysis of the polymers in THF relative to narrow polystyrene standards gave molecular weight estimates of M_n = 29,480 ($Đ$ = 2.34) for **P1** and M_n = 16,680 ($Đ$ = 1.47) for **P2**, corresponding to number-average degrees of polymerization of DP_n = 30 and 10 respectively. The difference in molecular weight is

consistent with ^{1}H NMR data that show signals between 7.9–8.0 ppm attributed to BTD end groups; these signals are more prominent for **P2**. The higher molecular weight of **P1** may be a result of the better solubilizing effect of the ethyl groups on boron compared with the pentafluorophenyl groups.

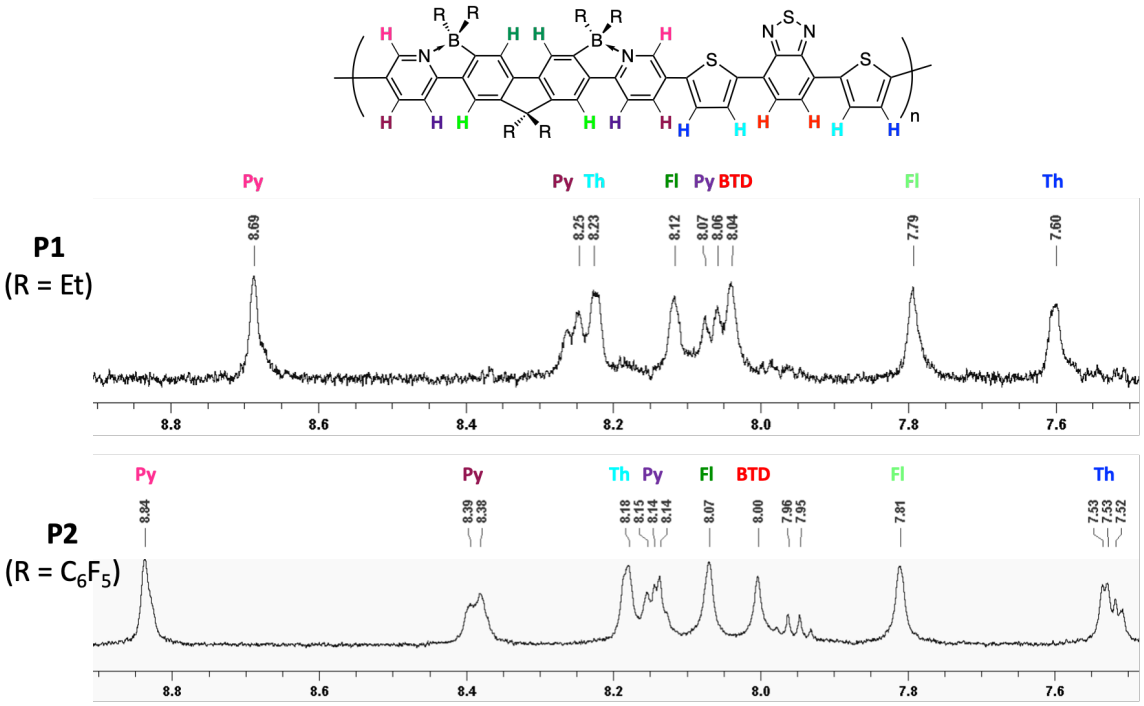

Figure 2. Aromatic regions of the ^{1}H NMR spectra of copolymers **P1** and **P2** showing assignments based on 2D H,H-COSY, H,H-TOCSY and H,H-NOESY NMR spectra of **P2**.

To investigate the electronic structure of the polymers, cyclic voltammetry measurements were performed on thin films of **P1** and **P2** in anhydrous acetonitrile containing 0.1 M $Bu_4N[PF_6]$ as the supporting electrolyte. **P1** showed two reversible redox waves at $E_{½}$ = -1.54 V and -1.94 V relative to the ferrocene/ferrocenium redox couple (Figure 3). The redox potential of **P1** is less negative than that of the previously reported homopolymer Poly(BNEt)[39], for which the first reduction occurred at $E_{½}$ = -2.31 V. This is consistent with a lower LUMO of copolymer **P1** as a result of incorporation of BTDDT as comonomer. The reductions for **P2** were shifted to even less negative potentials of $E_{½}$ = -1.51 V and -1.85 V. This indicates that the LUMO level for **P2** is relatively even lower than that of **P1** because of the electron-withdrawing effect of the pentafluorophenyl groups on boron.

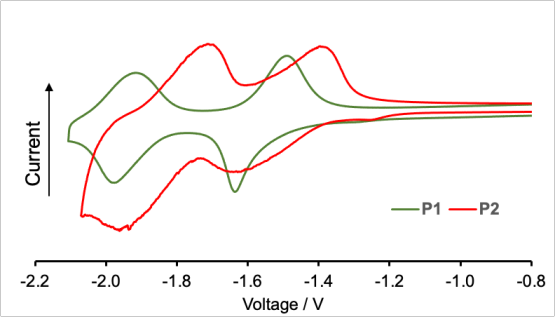

Figure 3. Cyclic voltammograms of **P1** and **P2** as thin films in acetonitrile containing 0.1 M $Bu_4N[PF_6]$ (scan rate 250 mV s^{-1}); reported relative to Fc/Fc^+.

These trends were further confirmed by DFT calculations on the borane monomers BNMe' and BNPf' (Br replaced by H, Et replaced by Me) and the corresponding model dyads BNMe'-BTDDT and BNPf'-BTDDT (Figure 4). For comparison, we also performed computations on the respective carbonaceous monomer CCMe' in which B and N are replaced by carbons and its dyad CCMe'-BTDDT (Supporting Information). For both BNMe' and BNPf', the HOMO is mostly localized on the fluorene moiety whereas the LUMO shows contributions from both the fluorene and pyridyl moieties. The orbital distribution is similar to that of CCMe' but the HOMO for BNMe' and BNPf' is more strongly localized on the central fluorene moieties. The HOMO energy decreases in the order -5.11 eV (CCMe') > -5.40 eV (BNMe') > -5.98 eV (BNPf') and the effect on the LUMO energy is even more pronounced as it decreases in the order -1.28 eV (CCMe') > -1.88 eV (BNMe') > -2.52 eV (BNPf'). Thus, relative to the carbonaceous analog CCMe', the HOMO and especially the LUMO of the B-N ladders are much lower in energy, signifying the strong effect of B←N Lewis pair doping on the frontier orbital energies of the monomers. Further, the HOMO and LUMO of BNPf' are significantly lower in energy than those of BNMe', the effect being slightly larger for the LUMO, which demonstrates that the monomer electronic structure is strongly influenced by the exocyclic boron substituents.

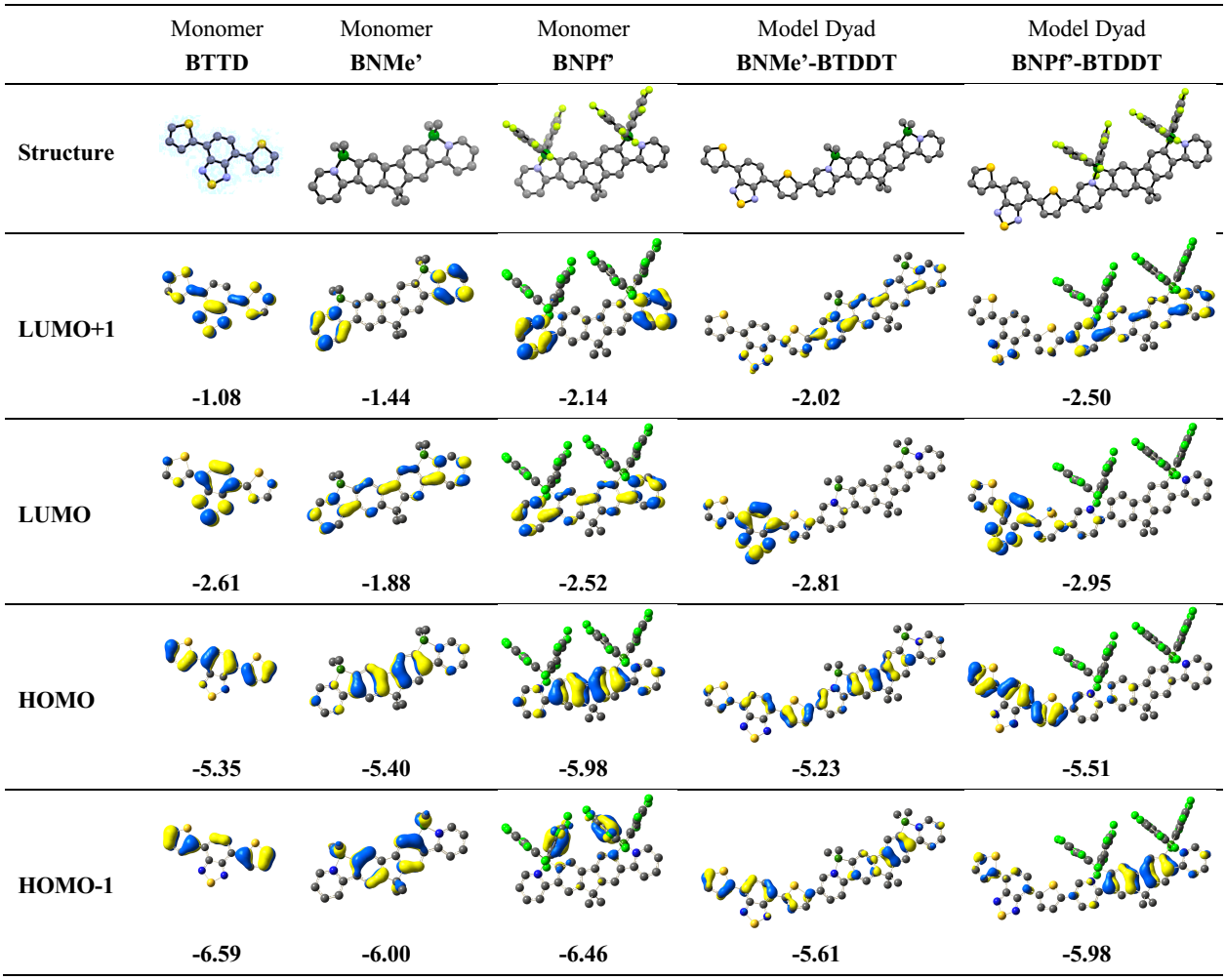

Figure 4. Kohn-Sham HOMO and LUMO orbital representations for monomers and model dyads (RB3LYP/6-31G(d), scaling radii of 75%, isovalue = 0.04, orbital energies given in eV). Br atoms were replaced by H atoms and Et groups by Me groups.

The HOMO and LUMO energy levels of the BTDDT unit (most stable *trans-trans* conformer [58]) were computed to be -2.61 eV and -5.35 eV. As illustrated in Figure 5, this places the HOMO level of BTDDT slightly below that of BNMe', similar in energy to that of BNMe' and significantly above that of BNPf'. On the other hand, the LUMO level of BTDDT is far below that of CCMe', well below that of BNMe' and just slightly below that of BNPf'. Attachment of the BTDDT moiety to give the dyads CCMe'-BTDDT, BNMe'-BTDDT and BNPf'-BTDDT results in orbital mixing, but the effect is drastically different for the three dyads. The HOMO for CCMe'-BTDDT and BNMe'-BTDDT is spread over the entire conjugated framework, but for BNPf'-BTDDT the HOMO is localized on the BTDDT and the HOMO-1 on the fluorene moiety.

This difference can be attributed to the energy mismatch of the HOMOs of BNPf' and BTDDT which is a consequence of the stronger electron-withdrawing effect of the $B(C_6F_5)_2$ groups on the dipyridylfluorene moiety. Further, whereas for CCMe'-BTDDT (-2.60 eV) the LUMO is virtually unchanged from that of BTDDT (-2.61 eV), the LUMO levels of BNMe'-BTDDT (-2.81 eV) and BNPf'-BTDDT (-2.95 eV) are shifted to lower energy, despite being localized primarily on the BTD acceptor, demonstrating the electron-withdrawing effect exerted by the B-N ladder monomers. The fact that the LUMO of BNPf'-BTDDT is relatively lower in energy than that of BNMe'-BTDDT further suggests that the substituents on boron influence the overall acceptor character of the polymer as also seen in the cyclic voltammetry data. The facile tunability of the HOMO and LUMO energy levels through simple substituent exchange on boron is remarkable as it typically requires design of entirely different monomer units.

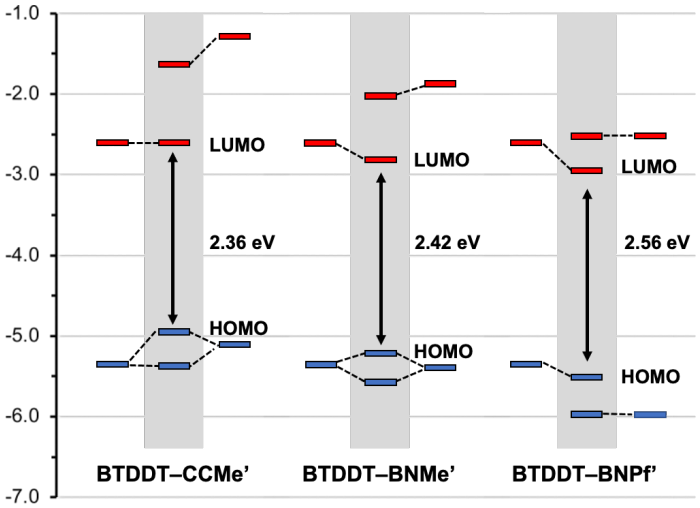

Figure 5. Computed frontier orbital energy levels for combinations of BTDDT with CCMe', BNMe', and BNPf' (DFT, RB3LYP/6-31G(d)), orbital energies given in V).

Because of the addition of the BTD moiety and ensuing lowering of the LUMO level, the HOMO-LUMO gap is greatly reduced in the dyads BNMe'-BTDDT (2.42 eV) and BNPf'-BTDDT (2.56 eV) relative to the boron monomers BNMe' (3.52 eV) and BNPf' (3.46 eV); it is also smaller than that of the BTDDT monomer itself (2.74 eV). The energy gap for the dyads slightly increases in the order CCMe'-BTDDT < BNMe'-BTDDT < BNPf'-BTDDT as the HOMO becomes more localized on the BTDDT unit and its relative energy decreases.[59] Nevertheless, a calculation on a dimer of the BNPf'-BTDDT dyad reveals that with further extension from the monomeric dyad

to a dimeric dyad (and ultimately the polymer) the LUMO further decreases in energy and so does the HOMO-LUMO gap (Figure S25).

The absorption and emission spectra of monomers BNEt and BNPf, BTDDT[58,60,61], and copolymers **P1** and **P2** in THF solution are displayed in Figure 6, and the data are summarized in Table 1. Monomers BNEt and BNPf show absorption maxima at 408 nm and 416 nm and emission maxima at 420 nm and 451 nm, respectively, while those of BTDDT[58,60,61] appear at 448 nm and 575 nm. The absorption and emission bands of the polymers are shifted to longer wavelengths, as **P1** and **P2** show absorption maxima at 516 nm and 508 nm and emission maxima at 641 nm and 627 nm respectively. The redshift is slightly less pronounced than for the all-carbon based polymer **B** (λ_{Abs} = 421, 544 nm in chlorobenzene [53]), which is consistent with our DFT studies on the model dyads. A comparison with the absorption and emission maxima of the homopolymer Poly(BNEt)[39] (λ_{Abs} = 458 nm, λ_{Em} = 472 nm) confirms that the reduction of the HOMO-LUMO gap relatively to the boron monomers is directly related to the incorporation of the BTDDT co-monomer. Incorporation of the electron-deficient BTD co-monomer leads to a lower LUMO level and in turn a reduced optical energy gap, which is estimated to be 2.11 eV (**P1**) and 2.16 eV (**P2**) based on the absorption onsets (2.58 eV for Poly(BNEt)[39]). Although the LUMO level of **P1** was determined electrochemically to be relatively higher than that of **P2**, the absorption and emission maxima of **P1** are slightly shifted to lower energy due to a relatively higher HOMO as indicated by the computational studies.

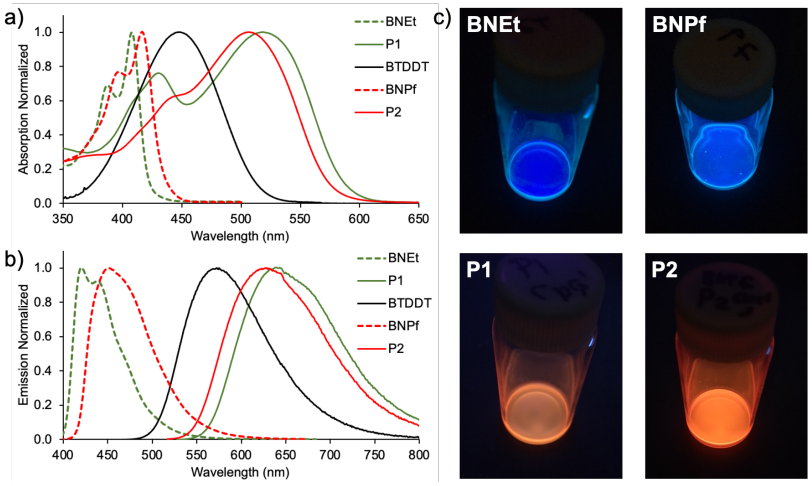

Figure 6. a) UV–vis absorption and b) emission spectra of **P1** and **P2** in comparison to monomers BNEt, BNPf, and BTDDT in THF solution; c) photographs of $CHCl_3$ solutions of monomers BNEt, BNPf (top) and polymers **P1**, **P2** (bottom) under UV light irradiation (365 nm).

Table 1. Photophysical properties of polymers **P1** and **P2** in comparison to monomers[a]

Compd	λ_{Abs} / nm	λ_{Em} / nm [b]	ϕ_{Fl} / % [c]	τ_{Fl} / ns [d]	k_r [e] / 10^8 s^{-1}	k_{nr} [e] / 10^8 s^{-1}
BTDDT	448	575	75	13.3	0.56	0.19
BNEt[39]	408	420	31.7	1.2	2.7	5.8
P1	516, 430	641	56.0	2.7[f]	2.1	1.6
BNPf	416	451	41.6	0.89	4.7	6.6
P2	508, 443 (sh)	627	54.3	2.1[f]	2.6	2.2

[a] In 10 μM THF solution; [b] excited at longest wavelength absorption maximum; [c] absolute quantum yield determined using an integrating sphere; [d] data from single exponential fits (excitation at 450 nm); [e] radiative (k_r) and non-radiative (k_{nr}) decay rate constants are calculated using the equations $k_r = \Phi / \tau$, $k_{nr} = (1 - \Phi) / \tau$; [f] average of double-exponential fit.

TD-DFT data for the model dyads (Table S5, Supporting Information) reveal that the lowest energy transition is primarily due to HOMO-to-LUMO excitation for BNPf'-BTDDT but shows a relatively more prominent HOMO-1-to-LUMO component for BNMe'-BTDDT. The lowest energy transition of BNMe'-BTDDT is then best described as a transition from a highly delocalized set of orbitals to the BTD acceptor unit. In contrast, for BNPf'-BTDDT, the lowest energy transition is largely localized on the BTDDT entity. For both dyads, an intense higher energy transition is seen that primarily involves charge transfer to the borylated dipyridylfluorene (LUMO+1) rather than the BTD (LUMO) moiety.

When excited at their absorption maxima, the polymers give rise to a strong orange fluorescence in THF solution with quantum yields of 56.0% (**P1**) and 54.3% (**P2**) respectively, that exceed those of the blue-emissive monomers BNMe and BNPf, as well as that of BTDDT (Table 1). The high quantum yields are accompanied by lifetimes of ca. 2–3 ns that are relatively longer than those of the boron monomers (~1 ns), but much shorter than that of BTDDT (~13 ns). The strong emission is attributed to the rigid structure of the polymer that favors radiative over non-radiative decay, despite the relatively small band gaps. The comparatively higher non-radiative rate constants for the boron monomers are attributed in part to the presence of the bromine heavy atoms that may facilitate intersystem crossing (ISC) followed by non-radiative decay from triplet excited states.

Conclusions

A new class of copolymers is introduced that combines B-N Lewis pair-fused dipyridylfluorene and ambipolar BTDDT units. The copolymers are obtained in modest yields by Pd-catalyzed Stille-type copolymerization. Taking advantage of the moderate solubility in toluene, low molecular weight oligomers were removed by extraction with toluene, providing the pure polymers with molecular weights of M_n = 29,480 ($Đ$ = 2.34) for **P1** and M_n = 16,680 ($Đ$ = 1.47) for **P2**. Relative to the respective monomers, as well as a previously reported homopolymer, Poly(BNEt), the absorptions and emissions are dramatically shifted to longer wavelengths, indicating effective extension of conjugation. Electrochemical measurements are consistent with a lowered LUMO level due to incorporation of BTD moieties into the polymer chains. This was confirmed by computational studies on model dyads that not only show that the LUMOs are centered primarily on the BTD moieties, but also that they are greatly decreased in comparison to those of an all-carbon analog and directly impacted by the electronic structure of the B-N ladder comonomers. Excitation with UV light gives rise to strong orange fluorescence in THF solution with maxima at 641 nm (R = Et) and 627 nm (R = C_6F_5) respectively. Overall, our results indicate that B-N Lewis pair-fused dipyridylfluorene ladder-type monomers are effective building blocks for the design of new conjugated copolymers with tunable band gaps and strong emission that could prove interesting for applications in areas ranging from organic electronics to fluorescent imaging of biological systems.

Acknowledgements. F.J. thanks the US National Science Foundation (NSF Grant CHE-1954122) and Rutgers University for support. The 500 MHz NMR spectrometers (NSF MRI 1229030, ELF III 047-04) were purchased with support from the NSF and the State of New Jersey. A.F.A. thanks the Saudi Arabia Government for a graduate fellowship. We thank Dr. Pavel Kucheryavy at Rutgers University-Newark for assistance with acquisition of 2D NMR data, Dr. Roman Brukh for assistance with acquisition of mass spectral data, and Dr. Monika Baraniak for assistance with GPC measurements.

References

1. Liu ZQ, Marder TB (2008) B-N versus C-C: How similar are they? Angew Chem Int Ed 47 242-244.
2. Helten H (2016) B=N Units as Part of Extended π-Conjugated Oligomers and Polymers. Chem - Eur J 22 12972-12982.
3. Giustra ZX, Liu SY (2018) The State of the Art in Azaborine Chemistry: New Synthetic Methods and Applications. J Am Chem Soc 140 1184-1194.
4. Bosdet MJD, Piers WE, Sorensen TS, Parvez M (2007) 10a-Aza-10b-borapyrenes: Heterocyclic analogues of pyrene with internalized BN moieties. Angew Chem, Int Ed 46 4940-4943.
5. Wang XY, Lin HR, Lei T, Yang DC, Zhuang FD, Wang JY, Yuan SC, Pei J (2013) Azaborine Compounds for Organic Field-Effect Transistors: Efficient Synthesis, Remarkable Stability, and BN Dipole Interactions. Angew Chem, Int Ed 52 3117-3120.
6. Wang XY, Wang JY, Pei J (2015) BN Heterosuperbenzenes: Synthesis and Properties. Chem Eur J 21 3528-3539.
7. Matsui K, Oda S, Yoshiura K, Nakajima K, Yasuda N, Hatakeyama T (2018) One-Shot Multiple Borylation toward BN-Doped Nanographenes. J Am Chem Soc 140 1195-1198.
8. Zhang PF, Zeng JC, Zhuang FD, Zhao KX, Sun ZH, Yao ZF, Lu Y, Wang XY, Wang JY, Pei J (2021) Parent B2N2-Perylenes with Different BN Orientations. Angew Chem Int Ed 60 23313-23319.
9. Ouadoudi O, Kaehler T, Bolte M, Lerner H-W, Wagner M (2021) One tool to bring them all: Au-catalyzed synthesis of B,O- and B,N-doped PAHs from boronic and borinic acids. Chem Sci 12 5898-5909.
10. Mellerup SK, Wang S (2019) Boron-Doped Molecules for Optoelectronics. Trends Chem 1 77-89.
11. Wakamiya A, Taniguchi T, Yamaguchi S (2006) Intramolecular B-N Coordination as a Scaffold for Electron-Transporting Materials: Synthesis and Properties of Boryl-Substituted Thienylthiazoles. Angew Chem Int Ed 45 3170-3173.
12. Li D, Zhang HY, Wang Y (2013) Four-coordinate organoboron compounds for organic light-emitting diodes (OLEDs). Chem Soc Rev 42 8416-8433.
13. Matsumoto T, Tanaka K, Tanaka K, Chujo Y (2015) Synthesis and characterization of heterofluorenes containing four-coordinated group 13 elements: theoretical and experimental analyses and comparison of structures, optical properties and electronic states. Dalton Trans 44 8697-8707.
14. Pais VF, Alcaide MM, Lopez-Rodriguez R, Collado D, Najera F, Perez-Inestrosa E, Alvarez E, Lassaletta JM, Fernandez R, Ros A, Pischel U (2015) Strongly Emissive and Photostable Four-Coordinate Organoboron N,C Chelates and Their Use in Fluorescence Microscopy. Chem Eur J 21 15369-15376.
15. Bachollet SPJT, Volz D, Fiser B, Munch S, Ronicke F, Carrillo J, Adams H, Schepers U, Gomez-Bengoa E, Brase S, Harrity JPA (2016) A Modular Class of Fluorescent Difluoroboranes: Synthesis, Structure, Optical Properties, Theoretical Calculations and Applications for Biological Imaging. Chem Eur J 22 12430-12438.
16. Shen CS, Srebro-Hooper M, Jean M, Vanthuyne N, Toupet L, Williams JAG, Torres AR, Riives AJ, Muller G, Autschbach J, Crassous J (2017) Synthesis and Chiroptical Properties of

Hexa-, Octa-, and Deca-azaborahelicenes: Influence of Helicene Size and of the Number of Boron Atoms. Chem Eur J 23 407-418.
17. Dash BP, Hamilton I, Tate DJ, Crossley DL, Kim JS, Ingleson MJ, Turner ML (2019) Benzoselenadiazole and benzotriazole directed electrophilic C-H borylation of conjugated donor-acceptor materials. J Mater Chem C 7 718-724.
18. Morgan MM, Nazari M, Pickl T, Rautiainen JM, Tuononen HM, Piers WE, Welch GC, Gelfand BS (2019) Boron-nitrogen substituted dihydroindeno[1,2-b]fluorene derivatives as acceptors in organic solar cells. Chem Commun 55 11095-11098.
19. Maar RR, Zhang RZ, Stephens DG, Ding ZF, Gilroy JB (2019) Near-Infrared Photoluminescence and Electrochemiluminescence from a Remarkably Simple Boron Difluoride Formazanate Dye. Angew Chem Int Ed 58 1052-1056.
20. Saotome S, Suenaga K, Tanaka K, Chujo Y (2020) Design for multi-step mechanochromic luminescence property by enhancement of environmental sensitivity in a solid-state emissive boron complex. Mater Chem Front 4 1781-1788.
21. Iqbal SA, Pahl J, Yuan K, Ingleson MJ (2020) Intramolecular (directed) electrophilic C-H borylation. Chem Soc Rev 49 4564-4591.
22. Haque A, Al-Balushi RA, Raithby PR, Khan MS (2020) Recent Advances in π-Conjugated NC-Chelate Organoboron Materials. Molecules 25 2645.
23. Vanga M, Sa S, Kumari A, Murali AC, Nayak P, Das R, Venkatasubbaiah K (2020) Synthesis of π-extended B <- N coordinated phenanthroimidazole dimers and their linear and nonlinear optical properties. Dalton Trans 49 7737-7746.
24. Sakamaki T, Nakamuro T, Yamashita K, Hirata K, Shang R, Nakamura E (2021) B2N2-Doped Dibenzo[a,m]Rubicene: Modular Synthesis, Properties, and Coordination-Induced Color Tunability. Chem Mater 33 5337-5344.
25. Full J, Panchal SP, Götz J, Krause A-M, Nowak-Król A (2021) Modular Synthesis of Organoboron Helically Chiral Compounds: Cutouts from Extended Helices. Angew Chem Int Ed 60 4350-4357.
26. Zhu CZ, Fang L (2018) Locking the Coplanar Conformation of π-Conjugated Molecules and Macromolecules Using Dynamic Noncovalent Bonds. Macromol Rapid Commun 39 1700241.
27. Koch R, Sun Y, Orthaber A, Pierik AJ, Pammer F (2020) Turn-on fluorescence sensors based on dynamic intramolecular N -> B-coordination. Org Chem Front 7 1437-1452.
28. Dou CD, Ding ZC, Zhang ZJ, Xie ZY, Liu J, Wang LX (2015) Developing Conjugated Polymers with High Electron Affinity by Replacing a C-C Unit with a B-N Unit. Angew Chem, Int Ed 54 3648-3652.
29. Zhao RY, Dou CD, Xie ZY, Liu J, Wang LX (2016) Polymer Acceptor Based on BN Units with Enhanced Electron Mobility for Efficient All-Polymer Solar Cells. Angew Chem Int Ed 55 5313-5317.
30. Barbon SM, Gilroy JB (2016) Boron difluoride formazanate copolymers with 9,9-di-n-hexylfluorene prepared by copper-catalyzed alkyne-azide cycloaddition chemistry. Polym Chem 7 3589-3598.
31. Grandl M, Schepper J, Maity S, Peukert A, von Hauff E, Pammer F (2019) N -> B Ladder Polymers Prepared by Postfunctionalization: Tuning of Electron Affinity and Evaluation as Acceptors in All-Polymer Solar Cells. Macromolecules 52 1013-1024.
32. Huang JH, Li YQ (2018) BN Embedded Polycyclic π-Conjugated Systems: Synthesis, Optoelectronic Properties, and Photovoltaic Applications. Front Chem 6 341.

33. Ohtani S, Nakamura M, Gon M, Tanaka K, Chujo Y (2020) Synthesis of fully-fused bisboron azomethine complexes and their conjugated polymers with solid-state near-infrared emission. Chem Commun 56 6575-6578.
34. Wakabayashi J, Gon M, Tanaka K, Chujo Y (2020) Near-Infrared Absorptive and Emissive Poly(p-phenylene vinylene) Derivative Containing Azobenzene–Boron Complexes. Macromolecules 53 4524-4532.
35. Xiang Y, Meng H, Yao Q, Chang Y, Yu H, Guo L, Xue Q, Zhan C, Huang J, Chen G (2020) B ← N Bridged Polymer Acceptors with 900 nm Absorption Edges Enabling High-Performance All-Polymer Solar Cells. Macromolecules 53 9529-9538.
36. Ito S, Gon M, Tanaka K, Chujo Y (2021) Recent developments in stimuli-responsive luminescent polymers composed of boron compounds. Polym Chem 12 6372-6380.
37. Yusuf M, Liu KL, Guo F, Lalancette RA, Jäkle F (2016) Luminescent organoboron ladder compounds via directed electrophilic aromatic C-H borylation. Dalton Trans 45 4580-4587.
38. Liu KL, Lalancette RA, Jäkle F (2017) B-N Lewis Pair Functionalization of Anthracene: Structural Dynamics, Optoelectronic Properties, and O_2 Sensitization. J Am Chem Soc 139 18170-18173.
39. Alahmadi AF, Lalancette RA, Jäkle F (2018) Highly Luminescent Ladderized Fluorene Copolymers Based on B-N Lewis Pair Functionalization. Macromol Rapid Comm 39 1800456.
40. Liu KL, Lalancette RA, Jäkle F (2019) Tuning the Structure and Electronic Properties of B-N Fused Dipyridylanthracene and Implications on the Self-Sensitized Reactivity with Singlet Oxygen. J Am Chem Soc 141 7453-7462.
41. Vanga M, Lalancette RA, Jäkle F (2019) Controlling the Optoelectronic Properties of Pyrene by Regioselective Lewis Base-Directed Electrophilic Aromatic Borylation. Chem - Eur J 25 10133-10140.
42. Vanga M, Sahoo A, Lalancette RA, Jäkle F (2022) Linear Extension of Anthracene via B <- N Lewis Pair Formation: Effects on Optoelectronic Properties and Singlet O_2 Sensitization. Angew Chem Int Ed 61 e202113075.
43. Culver EW, Anderson TE, Navarrete JTL, Delgado MCR, Rasmussen SC (2018) Poly(thieno[3,4-b]pyrazine-alt-2,1,3-benzothiadiazole)s: A New Design Paradigm in Low Band Gap Polymers. ACS Macro Lett 7 1215-1219.
44. Anderson TE, Culver EW, Badia-Dominguez I, Wilcox WD, Buysse CE, Delgado MCR, Rasmussen SC (2021) Probing the nature of donor-acceptor effects in conjugated materials: a joint experimental and computational study of model conjugated oligomers. Phys Chem Chem Phys 23 26534-26546.
45. Kim Y, Cook S, Choulis SA, Nelson J, Durrant JR, Bradley DDC (2004) Organic Photovoltaic Devices Based on Blends of Regioregular Poly(3-hexylthiophene) and Poly(9,9-dioctylfluorene-co-benzothiadiazole). Chem Mater 16 4812-4818.
46. Nakashima M, Otsura T, Naito H, Ohshita J (2015) Synthesis of new D-A polymers containing disilanobithiophene donor and application to bulk heterojunction polymer solar cells. Polym J 47 733-738.
47. Fujiki M, Yoshimoto S (2017) Time-evolved, far-red, circularly polarised luminescent polymer aggregates endowed with sacrificial helical Si-Si bond polymers. Mater Chem Front 1 1773-1785.
48. Fei ZP, Han Y, Gann E, Hodsden T, Chesman ASR, McNeill CR, Anthopoulos TD, Heeney M (2017) Alkylated Selenophene-Based Ladder-Type Monomers via a Facile Route for High-Performance Thin-Film Transistor Applications. J Am Chem Soc 139 8552-8561.

49. Su YW, Lin YC, Wei KH (2017) Evolving molecular architectures of donor-acceptor conjugated polymers for photovoltaic applications: from one-dimensional to branched to two-dimensional structures. J Mater Chem A 5 24051-24075.
50. Wang Y, Shi L, Ye Z, Guan K, Teng L, Wu J, Yin X, Song G, Zhang X-B (2020) Reactive Oxygen Correlated Chemiluminescent Imaging of a Semiconducting Polymer Nanoplatform for Monitoring Chemodynamic Therapy. Nano Lett 20 176-183.
51. Liu A, Gedda L, Axelsson M, Pavliuk M, Edwards K, Hammarstroem L, Tian H (2021) Panchromatic Ternary Polymer Dots Involving Sub-Picosecond Energy and Charge Transfer for Efficient and Stable Photocatalytic Hydrogen Evolution. J Am Chem Soc 143 2875-2885.
52. Li M, Huang X, Ren J (2021) Multicolor Chemiluminescent Resonance Energy-Transfer System for In Vivo High-Contrast and Targeted Imaging. Anal Chem 93 3042-3051.
53. Wang M, Qin H, Wang L, Wei J, Cai D, Yin Z, Ma Y, Chen S-C, Tanga C, Zheng Q (2015) Ladder-type tetra-p-phenylene-based copolymers for efficient polymer solar cells with open-circuit voltages approaching 1.1 V. J Mater Chem A 3 21672-21681.
54. Sundararaman A, Jäkle F (2003) A Comparative Study of Base-Free Arylcopper Reagents for the Transfer of Aryl Groups to Boron Halides. J Organomet Chem 681 134-142.
55. Sundararaman A, Lalancette RA, Zakharov LN, Rheingold AL, Jäkle F (2003) Structural Diversity of Pentafluorophenylcopper Complexes. First Evidence of π-Coordination of Unsupported Arenes to Organocopper Aggregates. Organometallics 22 3526-3532.
56. Eggert Carlé J, Andreasen JW, Jørgensen M, Krebs FC (2010) Low band gap polymers based on 1,4-dialkoxybenzene, thiophene, bithiophene donors and the benzothiadiazole acceptor. Sol Energy Mater Sol Cells 94 774-780.
57. M. J. Frisch, G. W. Trucks, H. B. Schlegel, G. E. Scuseria, M. A. Robb, J. R. Cheeseman, G. Scalmani, V. Barone, G. A. Petersson, H. Nakatsuji, X. Li, M. Caricato, A. V. Marenich, J. Bloino, B. G. Janesko, R. Gomperts, B. Mennucci, H. P. Hratchian, J. V. Ortiz, A. F. Izmaylov, J. L. Sonnenberg, D. Williams-Young, F. Ding, F. Lipparini, F. Egidi, J. Goings, B. Peng, A. Petrone, T. Henderson, D. Ranasinghe, V. G. Zakrzewski, J. Gao, N. Rega, G. Zheng, W. Liang, M. Hada, M. Ehara, K. Toyota, R. Fukuda, J. Hasegawa, M. Ishida, T. Nakajima, Y. Honda, O. Kitao, H. Nakai, T. Vreven, K. Throssell, J. A. Montgomery, Jr., J. E. Peralta, F. Ogliaro, M. J. Bearpark, J. J. Heyd, E. N. Brothers, K. N. Kudin, V. N. Staroverov, T. A. Keith, R. Kobayashi, J. Normand, K. Raghavachari, A. P. Rendell, J. C. Burant, S. S. Iyengar, J. Tomasi, M. Cossi, J. M. Millam, M. Klene, C. Adamo, R. Cammi, J. W. Ochterski, R. L. Martin, K. Morokuma, O. Farkas, J. B. Foresman, and D. J. Fox, Gaussian 16, Revision A.03, Gaussian, Inc., Wallingford CT, 2016.
58. Nielsen CB, White AJP, McCulloch I (2015) Effect of Fluorination of 2,1,3-Benzothiadiazole. J Org Chem 80 5045-5048.
59. Köse ME (2019) Theoretical Estimation of Donor Strength of Common Conjugated Units for Organic Electronics. J Phys Chem A 123 5566-5573.
60. Iagatti A, Patrizi B, Basagni A, Marcelli A, Alessi A, Zanardi S, Fusco R, Salvalaggio M, Bussotti L, Foggi P (2017) Photophysical properties and excited state dynamics of 4,7-dithien-2-yl-2,1,3-benzothiadiazole. Phys Chem Chem Phys 19 13604-13613.
61. Pati PB, Senanayak SP, Narayan KS, Zade SS (2013) Solution Processable Benzooxadiazole and Benzothiadiazole Based D-A-D Molecules with Chalcogenophene: Field Effect Transistor Study and Structure Property Relationship. ACS Appl Mater Interf 5 12460-12468.